

UNCLASSIFIED

AD 601 734

601 734

Processed by . . .

CLEARINGHOUSE

FOR FEDERAL SCIENTIFIC AND TECHNICAL INFORMATION

OF THE

U.S. DEPARTMENT OF COMMERCE



for . . .

DEFENSE DOCUMENTATION CENTER
DEFENSE SUPPLY AGENCY

UNCLASSIFIED

BEST AVAILABLE COPY

NOTICE TO DEFENSE DOCUMENTATION CENTER USERS

This document is being distributed by the Clearinghouse for Federal Scientific and Technical Information, Department of Commerce, as a result of a recent agreement between the Department of Defense (DOD) and the Department of Commerce (DOC).

The Clearinghouse is distributing unclassified, unlimited documents which are or have been announced in the Technical Abstract Bulletin (TAB) of the Defense Documentation Center.

The price does not apply for registered users of the DDC services.

EFFECTIVE AREA OF RING STIFFENERS
FOR AXIALLY SYMMETRIC SHELLS

by

R. D. Short

March 1964

Report 1894

TABLE OF CONTENTS

	Page
ABSTRACT	1
INTRODUCTION	1
DERIVATION	2
CONSTANT DISPLACEMENT.....	2
VARYING DISPLACEMENT.....	3
STRESSES	12
SUMMARY	16
REFERENCES	16
INITIAL DISTRIBUTION	17

LIST OF FIGURES

Figure 1 - Loading and Nomenclature of Ring Stiffener (Frame)	2
Figure 2 - Plots for Equation (2), $v = 0.25$	6
Figure 3 - Plots for Equation (2), $v = 0.30$	7
Figure 4 - Plots for Equation (2), $v = 0.35$	8
Figure 5 - Plots for Equation (29), $v = 0.25$	9
Figure 6 - Plots for Equation (29), $v = 0.30$	10
Figure 7 - Plots for Equation (29), $v = 0.35$	11
Figure 8 - Plots for Equations (33) and (34), $v = 0.25$	13
Figure 9 - Plots for Equations (33) and (34), $v = 0.30$	14
Figure 10 - Plots for Equations (33) and (34), $v = 0.35$	15

ABSTRACT

The effectiveness of T- and I-section ring stiffeners in axially symmetric shells undergoing axially symmetric deformations is examined under the assumption that the thicknesses of the shell and flanges and web of the stiffeners are small compared to the other dimensions. Curves are presented for obtaining the effective area and the flange stress of T-stiffeners. Approximate formulas for stiffeners with depth of stiffener small compared to the radius of the shell are also presented.

INTRODUCTION

In the works of Von Sander and Günther,¹ and Salerno and Palos² for determining the axisymmetric behavior of ring stiffened circular cylindrical shells under uniform pressure loading, the effect of placement of the stiffener (frame) away from the middle surface of the shell is not considered. Indeed it has become customary with many investigators to assume, arbitrarily as they have,^{1,2,3} that the effect of the frame is the same as if its entire area were in fact concentrated at the middle surface of the shell.

As early as the year 1935, however, Trilling⁴ had reexamined and used the classical Lamb formula for a thick cylinder to ascertain the true frame reaction. In 1956, Wilson⁵ derived an approximate effective frame area, A_0 , based on the assumption of constant deflection over the entire frame section. His solution results in the equation

$$A_0 = A(R/R_G)^2 \quad (1)$$

where A is the actual frame area, R is the radius of the shell, and R_G is the radius of the center of gravity of the frame. This solution based on this assumption, nevertheless, is in error because it fails to consider equilibrium. However, a brief outline of the proper solution which results in the correction factor R/R_G appears in a later analysis.⁶

Wilson obtains a more correct solution based upon the Lamb stress distribution for the web which he expects is not significantly different from Equation (1), but apparently, except for a single example, he has made no estimate of this difference.

The purpose of this report is to show that the effective frame area can be

References are listed on page 16.

represented by

$$A_0 = A(R/R_0)^n \quad (2)$$

where ν is Poisson's ratio, and n is less than or greater than $1 + 2\nu$, according as the frame is internal or external, and to present curves to facilitate computation of A_0 and the frame stress.

DERIVATION

CONSTANT DISPLACEMENT

Suppose that the frame (Figure 1) is loaded by a radial load, q per-unit-length, at the cylindrical shell with radius R_0 . Further assume that the effect of radial strain, ϵ_r , on the radial displacements, w , is small so that w may be assumed to be constant across the section. If the radial stress is also assumed negligible, the circumferential stress, σ_θ , is given by

$$\epsilon_\theta = -Ew/r \quad (3)$$

where r is the radius of a particular point of the section and E is Young's modulus. Then considering equilibrium

$$\oint \sigma_\theta dA = 0 \quad (4)$$

Proceeding with the method of Wilson we write

$$z = R_0 + z \quad (5)$$

and

$$\frac{z}{r} = \frac{1}{R_0} \left[1 - \frac{z}{R_0} + \left(\frac{z}{R_0} \right)^2 - \dots \right]. \quad (6)$$

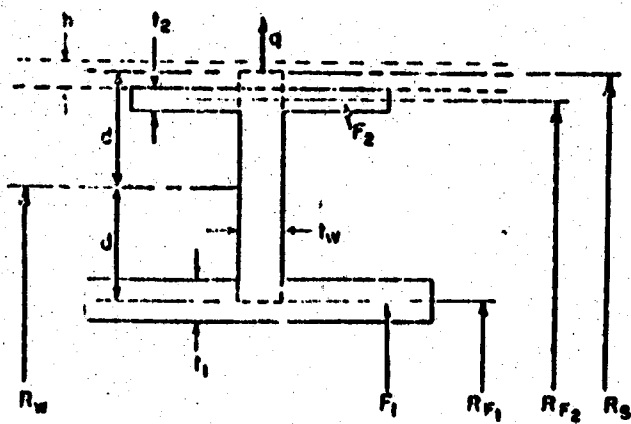


Figure 1 - Loading and Nomenclature of Ring Stiffener (Frame)

The integration indicated in Equation (4) may be performed by integrating piecewise over the frame and summing the results. Then if R_0 is taken as the radius to the center of gravity, R_i , of each piece so that $\int z dA$ vanishes for each piece,

$$qR_g = -Ew \sum_i (A_i/R_i) \left(1 + \frac{I_i}{A_i R_i^2} \right) \quad (7)$$

where A_i and I_i are the area and moment of inertia respectively of a piece.

The effective area is defined as

$$A_e = -qR_g^2 / (Ew). \quad (8)$$

Since the assumption of constant deflection is arbitrary and generally $I/(A_e R_g^2) \ll 1$, it is neglected and combination of Equations (7) and (5) yields

$$A_e = \sum_i A_i (R_g/R_i). \quad (9)$$

If no subdivision of the stiffener is made then Equation (9) reduces to Equation (2) with $n = 1$.

VARYING DISPLACEMENT

The assumption of constant w across the depth of a stiffener can be eliminated by application of the classical Lame thick cylinder analysis to the various components of the stiffener. However, for this method the thickness of the frame flanges and web will be assumed small compared to other dimensions and the effect of the three-dimensional stress condition at the junctures will be neglected.

First consider a simple rectangular ring of thickness, t , perpendicular to the radius, loaded externally by a tensile radial force, q_0 , per-unit-length at radius b and internally by tensile radial force, q_1 , per-unit-length at radius a . The radial deflections, w_b at the outside radius of the ring and w_a at the inside radius of the ring, are given by:

$$w_b = \frac{-bq_0}{Et} \left[\frac{b^2 + a^2 - v(b^2 - a^2)}{b^2 - a^2} \right] + \frac{2ba^2 q_1}{Et(b^2 - a^2)} \quad (10)$$

and

$$w_a = \frac{-2b^2 a q_0}{Et(b^2 - a^2)} + \frac{aq_1}{Et} \left[\frac{b^2 + a^2 + v(b^2 - a^2)}{b^2 - a^2} \right]. \quad (11)$$

By replacing $a + b$ by $2R_w$ and $(b - a)t$ by A_w Equations (10) and (11) can be written

$$w_b = \frac{-bq_0}{2EA_w R_w} (b^2 + a^2 - v(b^2 - a^2)) + \frac{ba^2 q_1}{EA_w R_w} \quad (12)$$

$$w_a = \frac{-b^2 a q_0}{EA_w R_w} + \frac{aq_1}{2EA_w R_w} (b^2 + a^2 + v(b^2 - a^2)). \quad (13)$$

If it is assumed that

$$w_a = \frac{-a^2 q_i}{EA_i} \quad (14)$$

which defines A_i as an effective flange area at $r = a$, then combining Equations (12), (13) and (14) will give

$$w_b = -\frac{bq_o}{E} \left\{ \frac{a[b^2 + a^2 - v(b^2 - a^2)] + (A_i/t)(b^2 - a^2)(1 - v^2)}{2A_w R_w a + A_i[b^2 + a^2 + v(b^2 - a^2)]} \right\}. \quad (15)$$

From Equations (8) and (15) the effective area at $r = b$ is

$$A_b = b \left\{ \frac{2A_w R_w a + A_i[b^2 + a^2 + v(b^2 - a^2)]}{a[b^2 + a^2 - v(b^2 - a^2)] + (A_i/t)(b^2 - a^2)(1 - v^2)} \right\}. \quad (16)$$

Now letting $b = R_w + d$ and $a = R_w - d$, Equation (16) reduces to:

$$A_b = \frac{A_w(b/R_w) + A_i(b/a)[1 + 2v(d/R_w) + (d/R_w)^2]}{1 - 2v(d/R_w) + (d/R_w)^2[1 + 4(1 - v^2)(R_w/a)(A_i/A_w)]}. \quad (17)$$

Similarly setting

$$w_b = \frac{b^2 q_o}{EA_o} \quad (18)$$

the effective area at $r = a$ is:

$$A_a = \frac{A_w(a/R_w) + A_o(a/b)[1 - 2v(d/R_w) + (d/R_w)^2]}{1 + 2v(d/R_w) + (d/R_w)^2[1 + 4(1 - v^2)(R_w/b)(A_o/A_w)]}. \quad (19)$$

If A_i and A_o are of the same order of magnitude as A_w and if d/R_w is sufficiently small so that $(d/R_w)^2$ can be neglected compared to 1, then

$$A_b \approx A_w(R_s/R_i)^{1+2v} + A_i(R_s/R_i)^{1+2v}. \quad (20)$$

It can be shown that within the same accuracy, i.e. $(d/R_w)^2 \ll 1$, Equation (20) is equivalent to

$$A_e = A(R_s/R_o)^{1+2v}. \quad (21)$$

This equation is the same as Equation (2) with $n = 1+2v$.

Equations (17) and (19) can now be applied to the internal frame in Figure 1 and a similar external frame, respectively resulting in

$$A_e = \frac{A_w(R_s/R_w) + A_{f1}(R_s/R_{f1}) [1 \pm 2v(d/R_w) + (d/R_w)^2]}{1 \pm 2v(d/R_w) + (d/R_w)^2 [1 + 4(1 - v^2)(R_w/R_{f1})(A_{f1}/A_w)]} + \\ A_{f2}(R_s/R_{f2})^{1+2v} \quad (22)$$

where A_{f2} includes only the outstanding legs of the faying flange and hence

$$R_w = \frac{1}{2}(R_s + R_{f1}) \quad (23)$$

and

$$d = \frac{1}{2}|R_s - R_{f1}|. \quad (24)$$

In Equation (22) and the equations that follow, the upper signs refer to external frames and the lower signs refer to internal frames.

Setting

$$\rho = 2d/R_s \pm \frac{\text{depth of frame}}{\text{radius of shell}} \quad (25)$$

$$R_w = R_s \pm d \quad \pm \text{radius to center of web} \quad (26)$$

and $K = A_{f1}/A_w$ (27)

and assuming a T-section hence

$$A_{f2} = 0,$$

then

$$R_0 = R_s \left[\frac{(1 \pm \rho/2) + K(1 \pm \rho)}{1 + K} \right] \quad (28)$$

and

$$\frac{A_e}{A} = \frac{1}{1+K} \left\{ \frac{\frac{2}{2 \pm \rho} + \frac{K}{1 \pm \rho} \left[1 \pm 2v \frac{\rho}{2 \pm \rho} + \left(\frac{\rho}{2 \pm \rho} \right)^2 \right]}{1 \pm 2v \frac{\rho}{2 \pm \rho} + \left(\frac{\rho}{2 \pm \rho} \right)^2 \left[1 + 2(1 - v^2) \frac{2 \pm \rho}{1 \pm \rho} K \right]} \right\}. \quad (29)$$

Plots of n in Equation (2) for a T-frame ($A_{f2} = 0$) as a function of ρ and K are presented in Figures 2, 3 and 4. The values of n for Figures 2, 3 and 4 are less than $1 + 2v$ for internal frames and greater than $1 + 2v$ for external frames. Plots of Equation (29) are presented in Figures 5, 6 and 7 to facilitate computation of A_e .

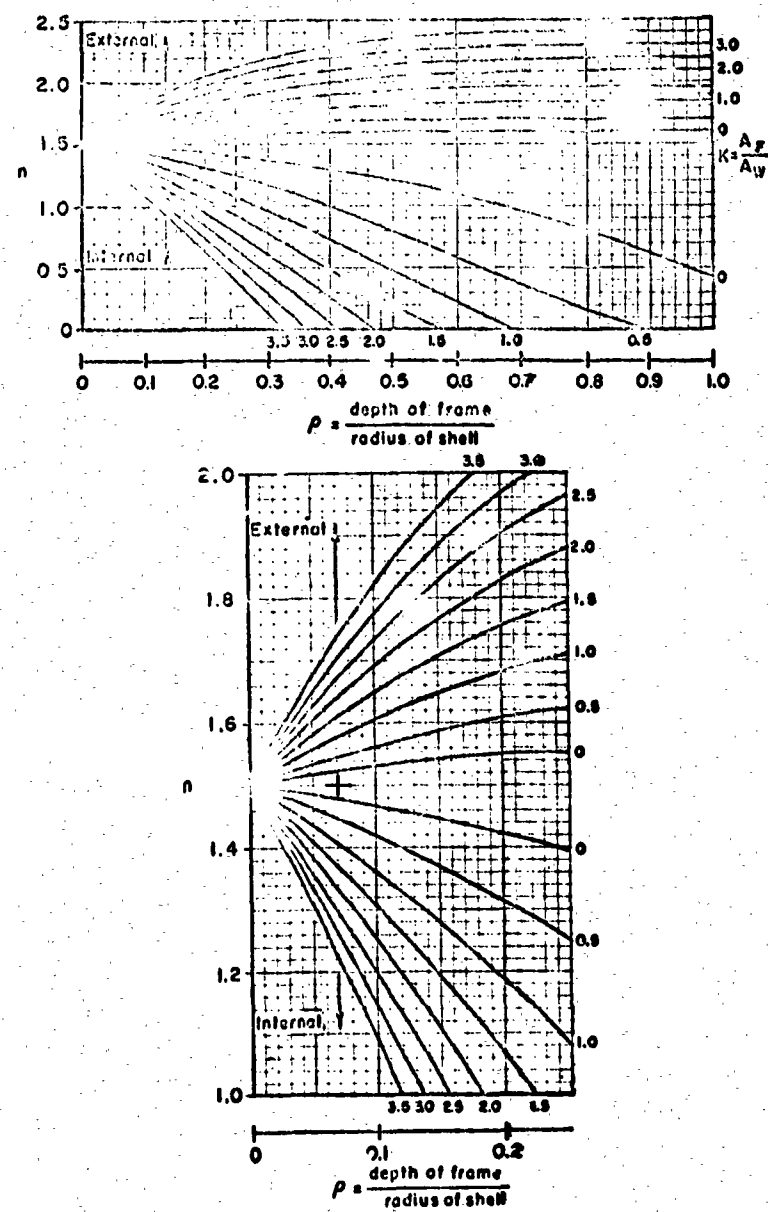


Figure 2 - Plots for Equation (2), $v = 0.25$

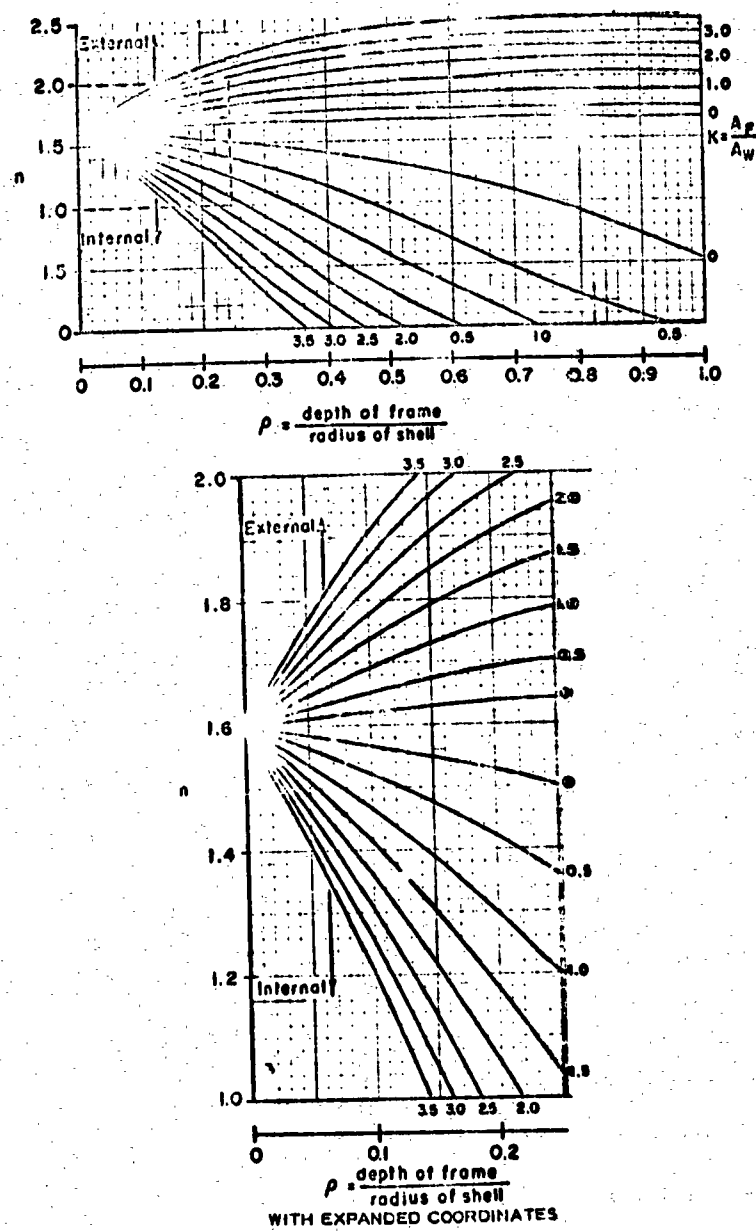


Figure 3 - Plots for Equation (2), $w = 0.30$

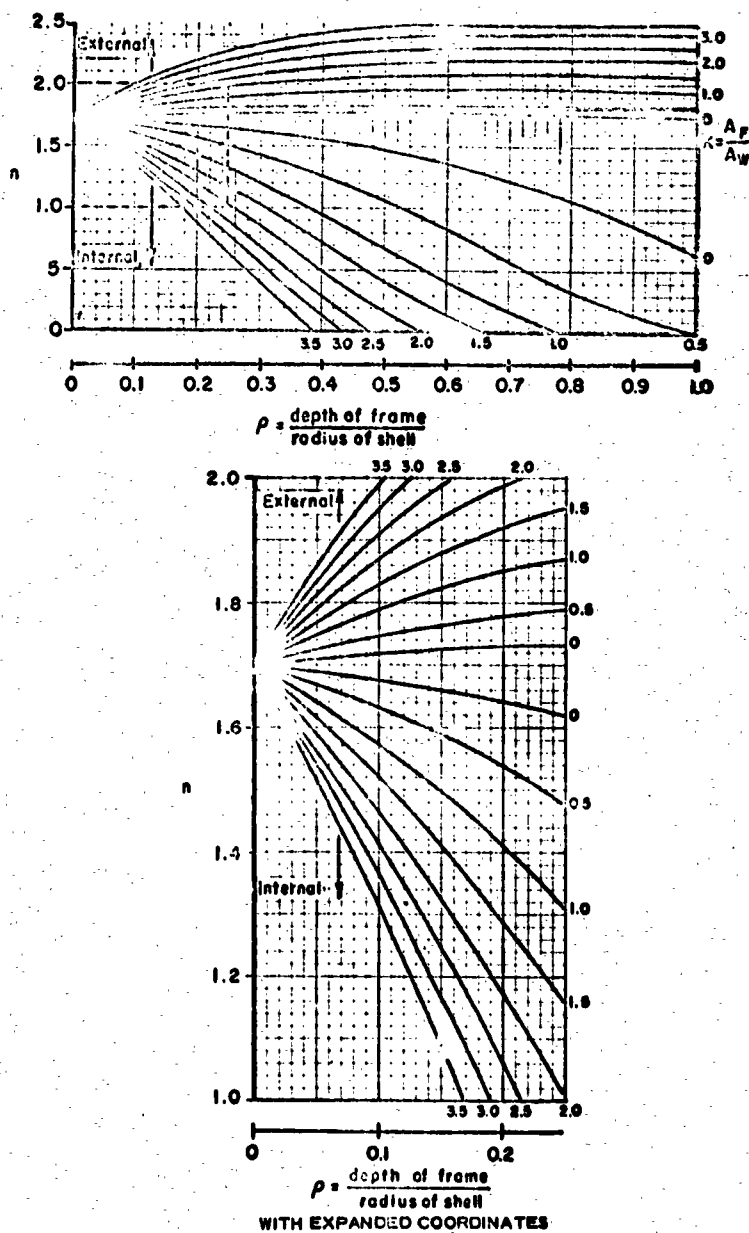
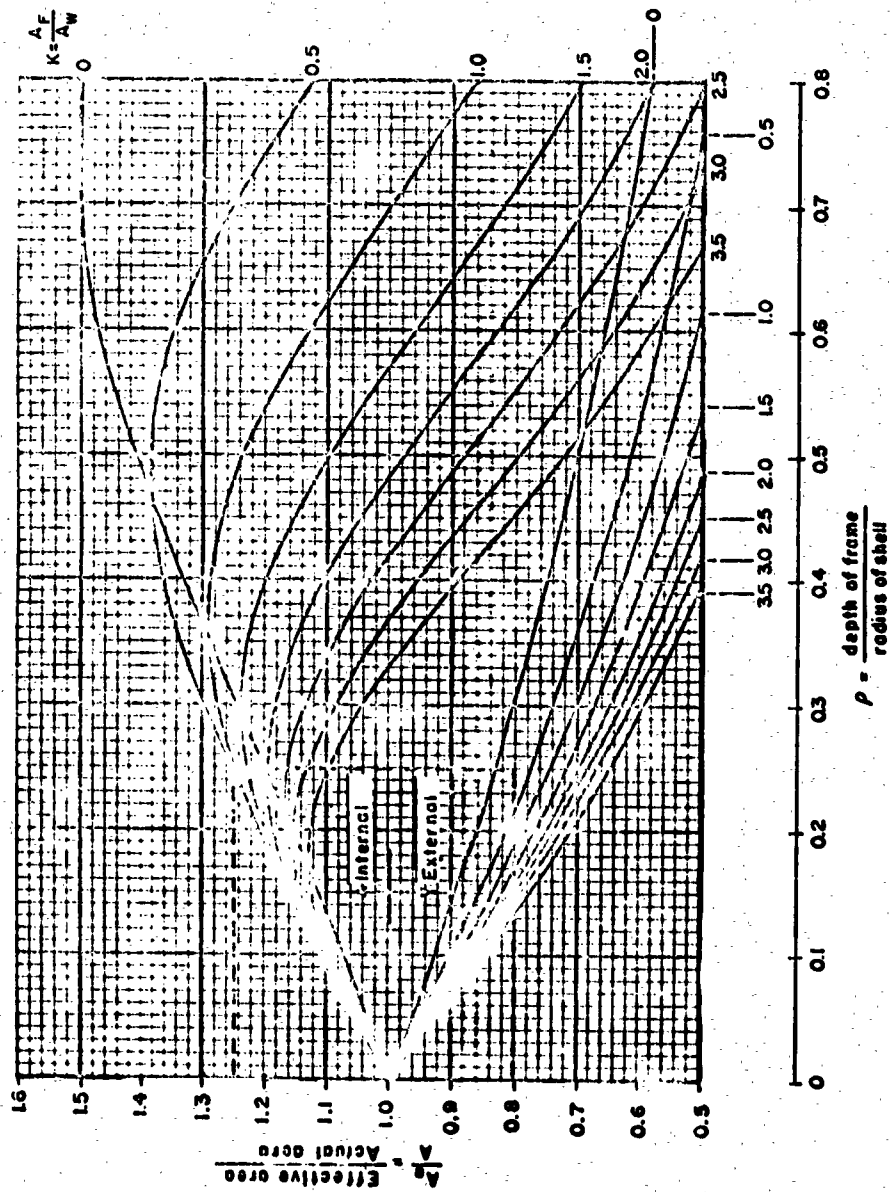


Figure 4 - Plots for Equation (2), $v = 0.35$



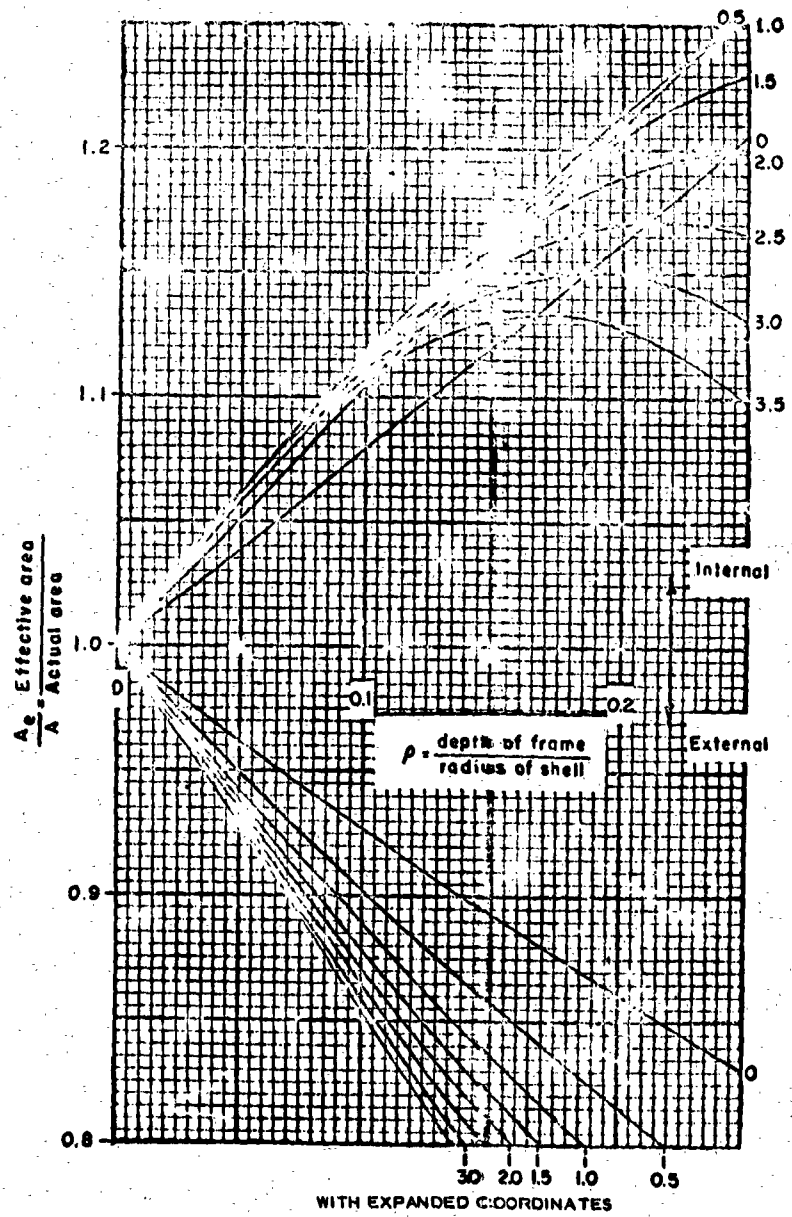
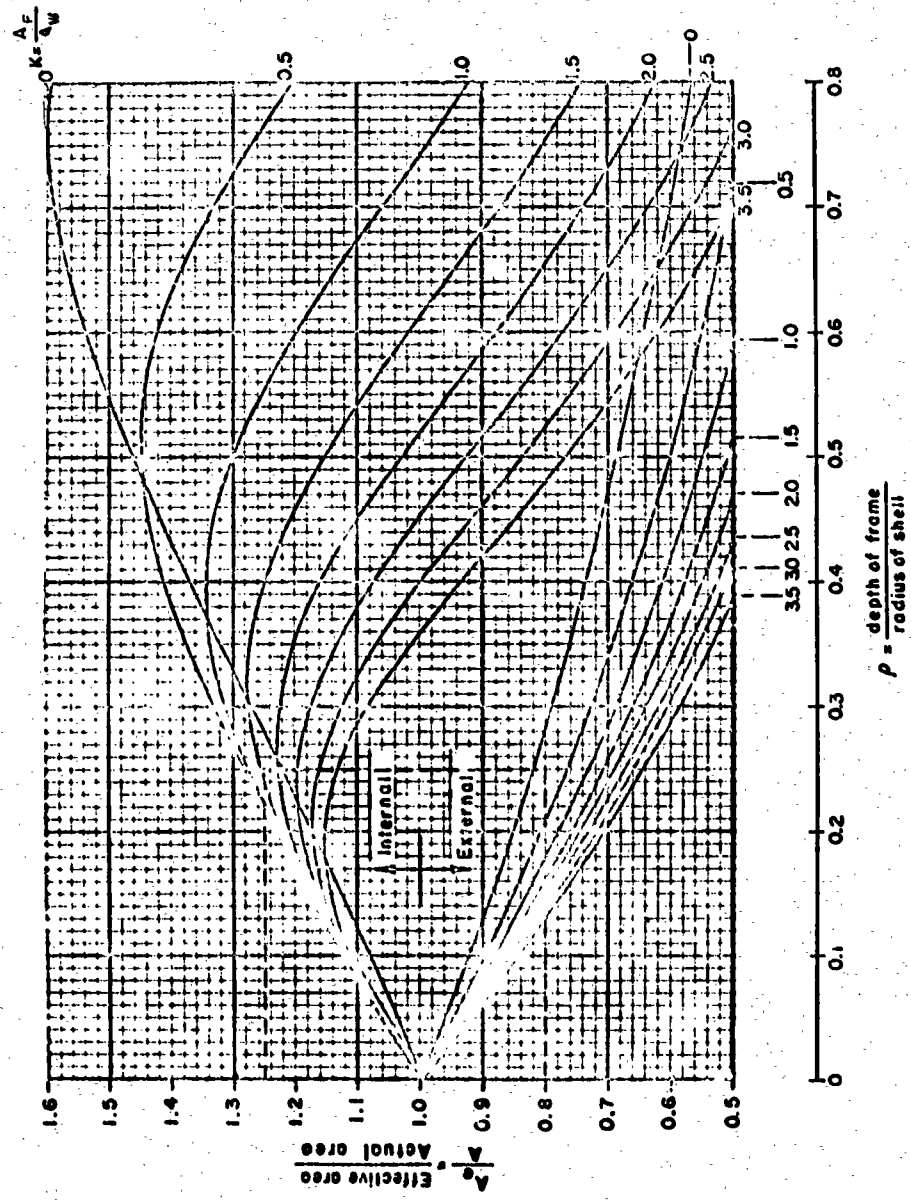


Figure 5 - Plots for Equation (29), $v = 0.25$



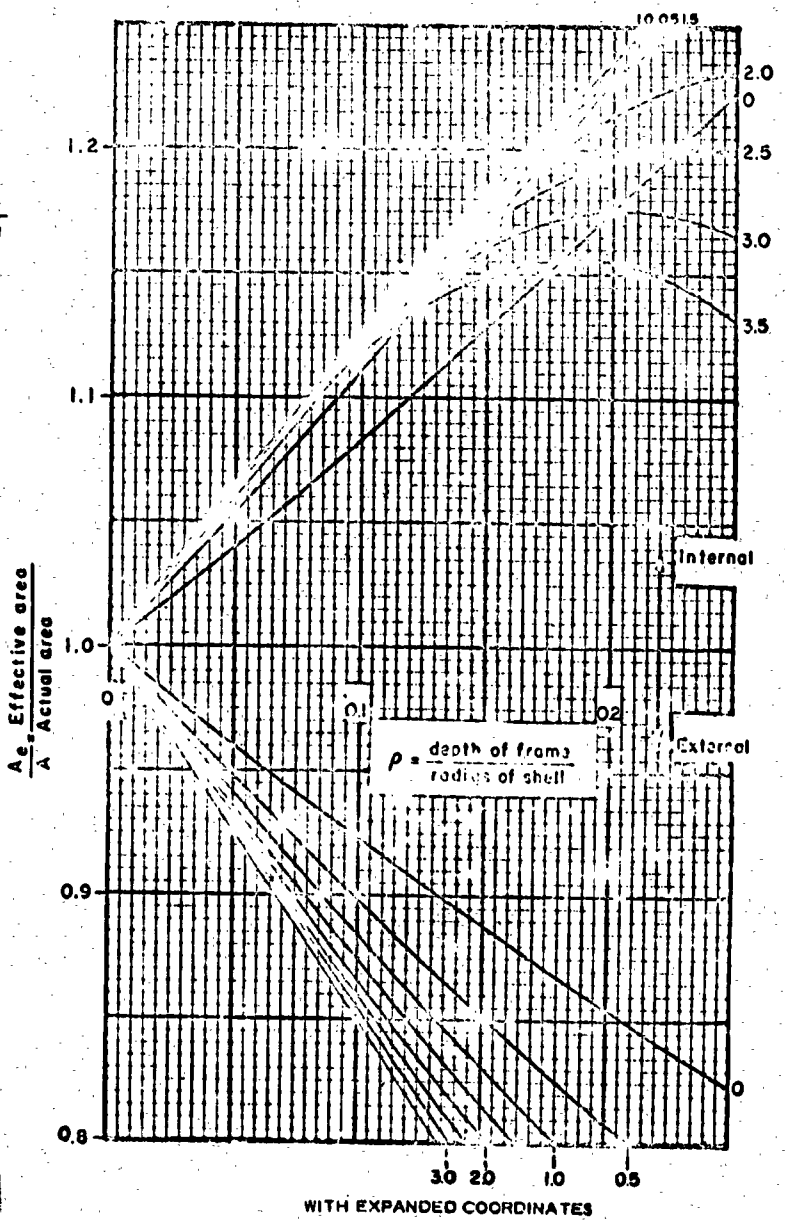
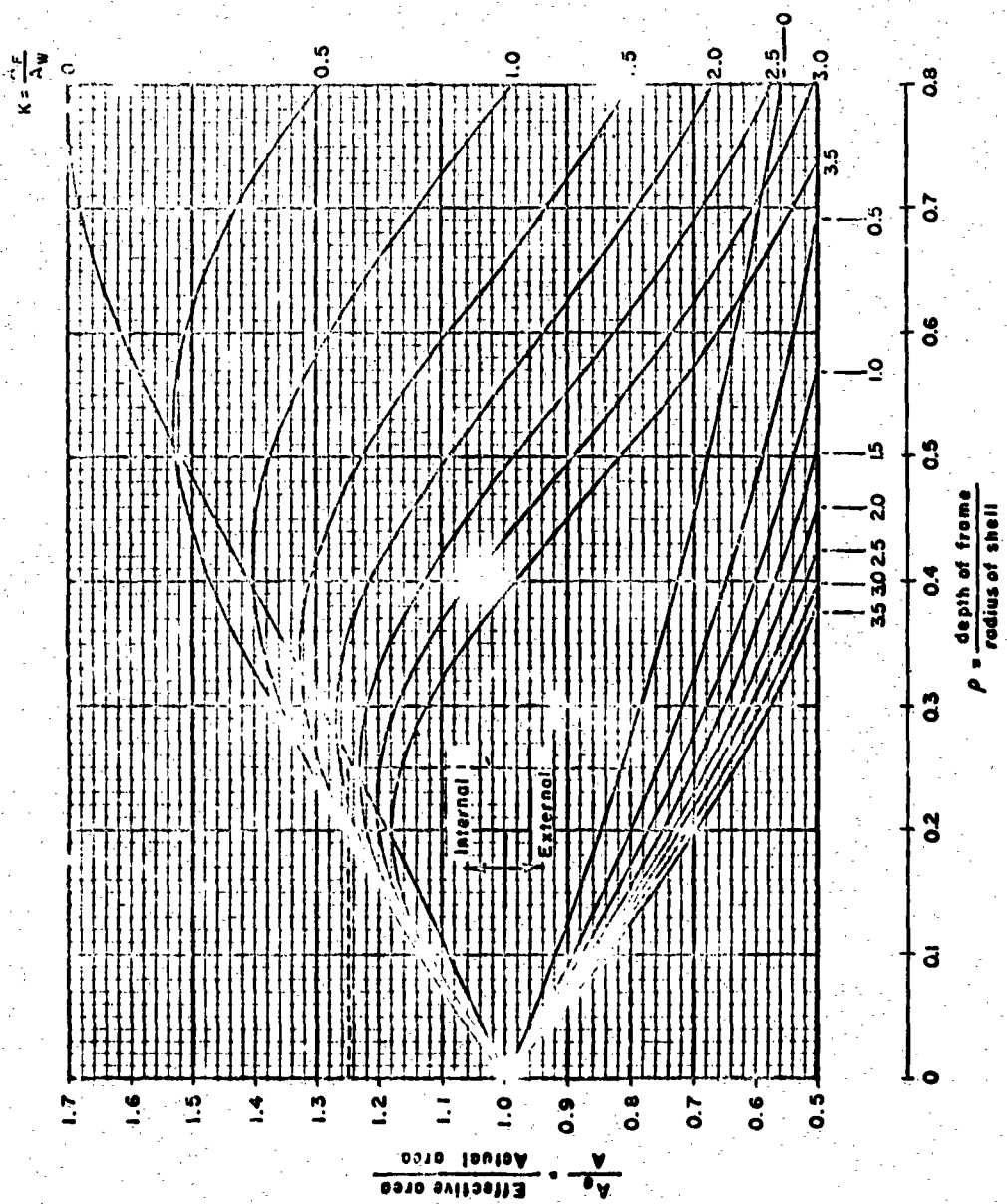


Figure 6 - Plots for Equation (29), $v = 0.30$



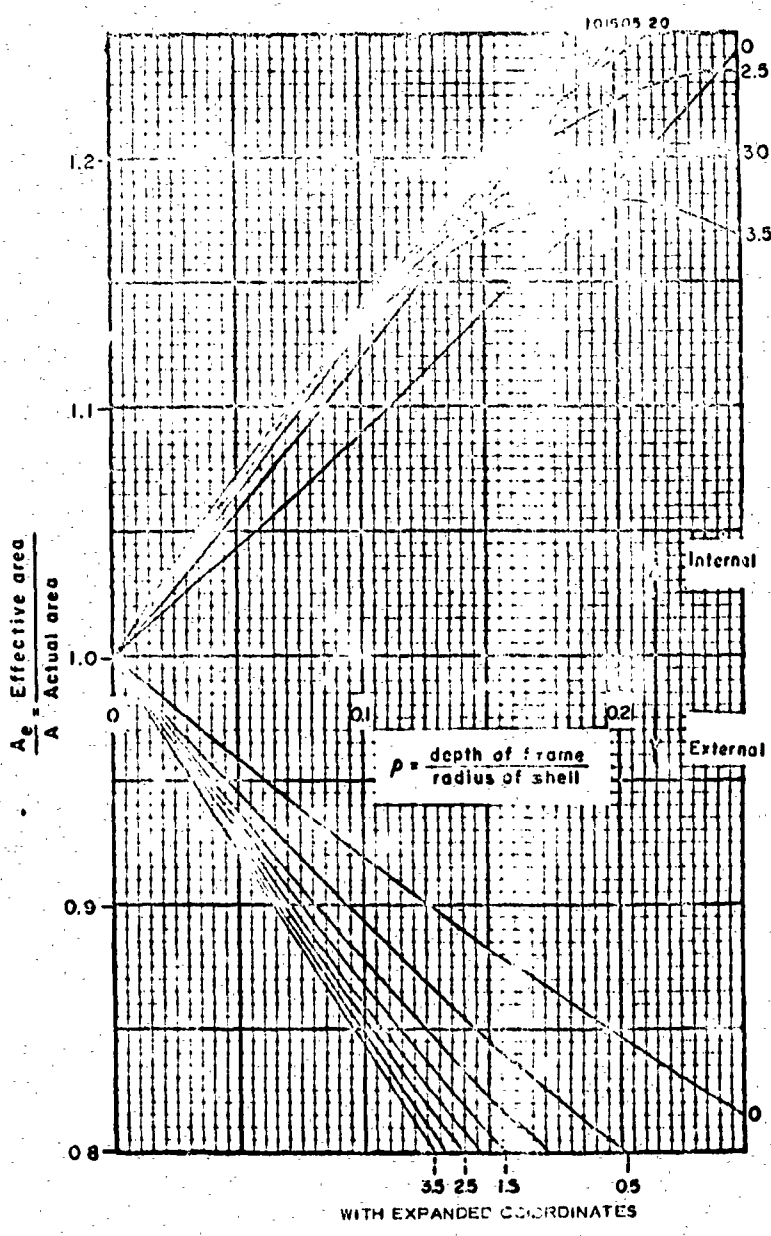


Figure 7 - Plots for Equation (29), $v = 0.35$

STRESSES

Increase of the effective frame area above the actual frame area implies a corresponding increase in the average frame stress. Hence, particularly for internal frames, knowledge of the frame flange stress is important in order to guard against premature frame failure. From Equations (13) and (14) the frame flange stress, σ_F , for an internal T-frame is:

$$\sigma_F = -\frac{Ew_F}{R_F} = +\frac{R_s^2 q_s}{A_w R_w} \cdot \frac{1}{1 + \frac{A_F}{2R_s R_w A_w} [R_s^2 + R_y^2 + v(R_s^2 - R_y^2)]} \quad (30)$$

The mean frame stress, σ_m , is

$$\sigma_m = \frac{R_s q_s}{A} \quad (31)$$

and the effective frame stress, σ_e , is

$$\sigma_e = R_s q_s / A_e \quad (32)$$

from which

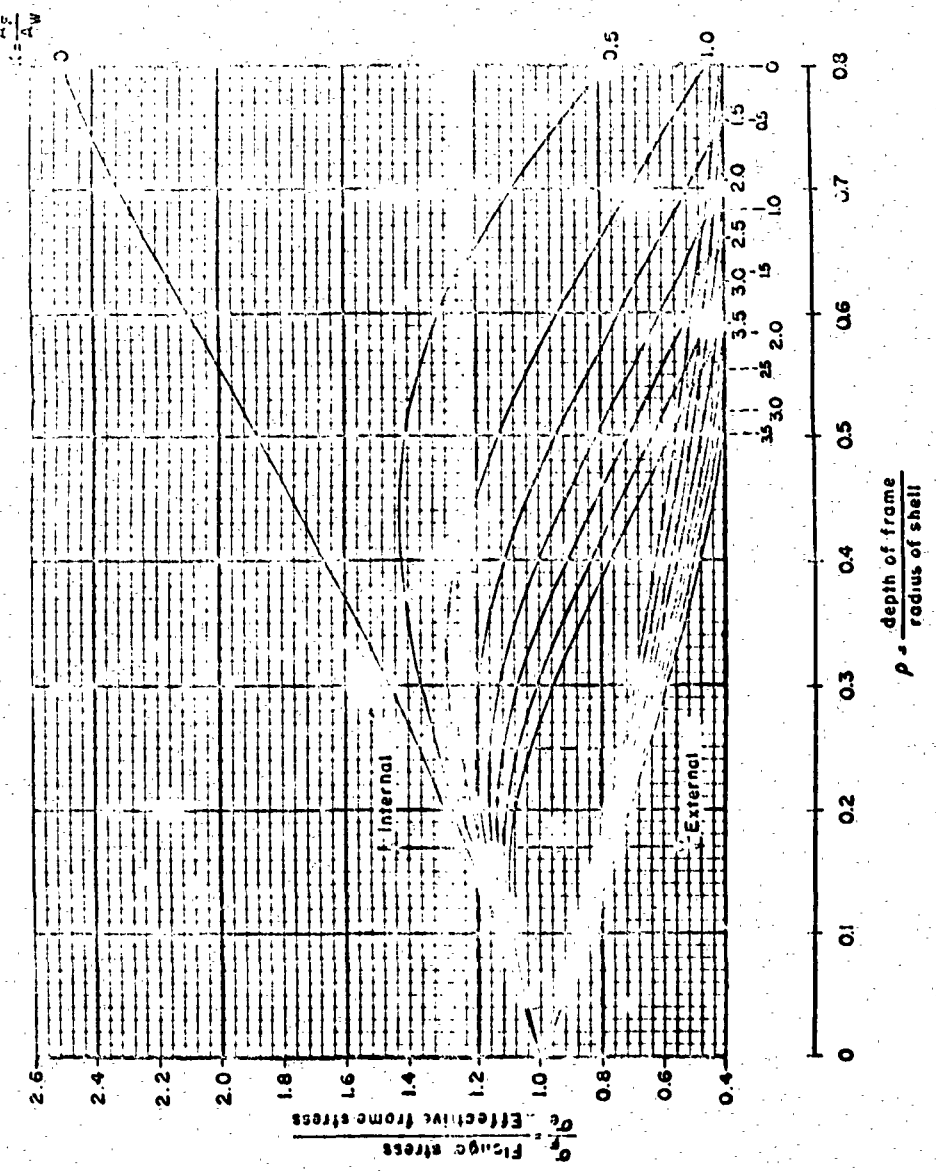
$$\sigma_F / \sigma_e = [2/(2-\rho)]^2 / [1 - 2v\rho/(2-\rho) + (\rho/(2-\rho))^2 [1 + 2(1-v^2)(2-\rho)K/(1-\rho)]] \quad (33)$$

Similarly for external frames

$$\sigma_F / \sigma_e = [2/(2+\rho)]^2 / [1 + 2v\rho/(2+\rho) + (\rho/(2+\rho))^2 [1 + 2(1-v^2)(2+\rho)K/(1+\rho)]] \quad (34)$$

Plots of Equations (33) and (34) are presented in Figures 8, 9 and 10. An approximation similar to that for Equation (21) gives

$$\sigma_F / \sigma_e = (R_s / R_p)^{1/v} \quad (35)$$



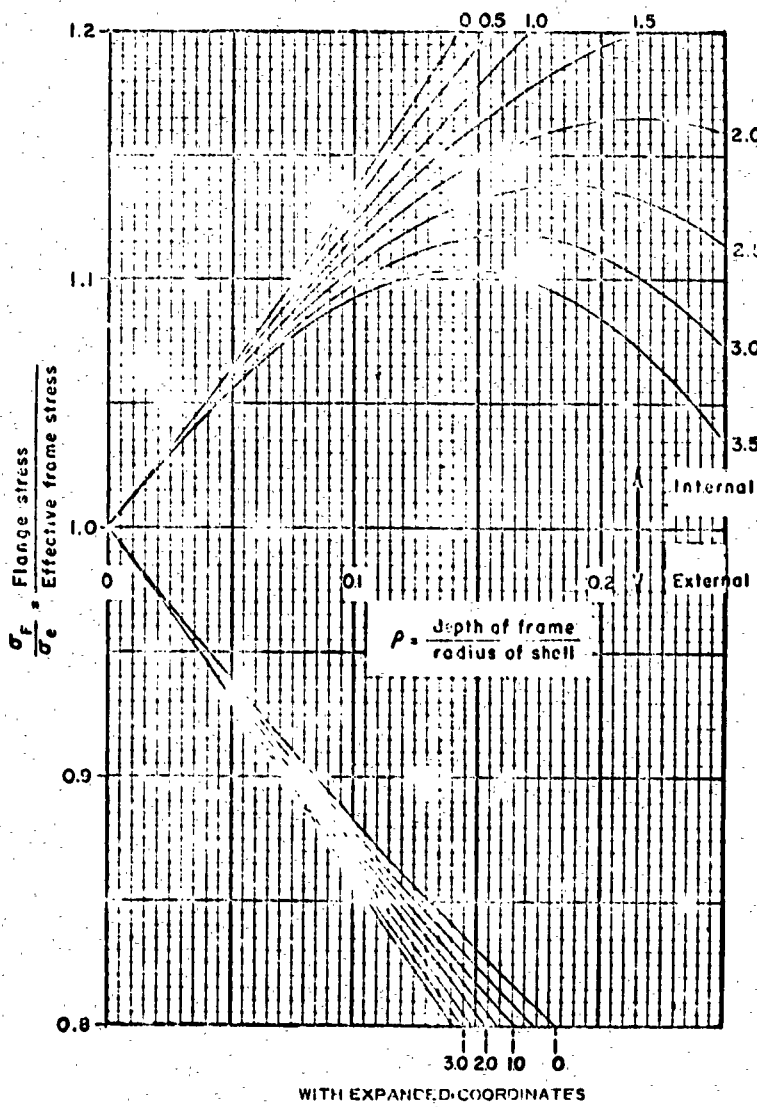
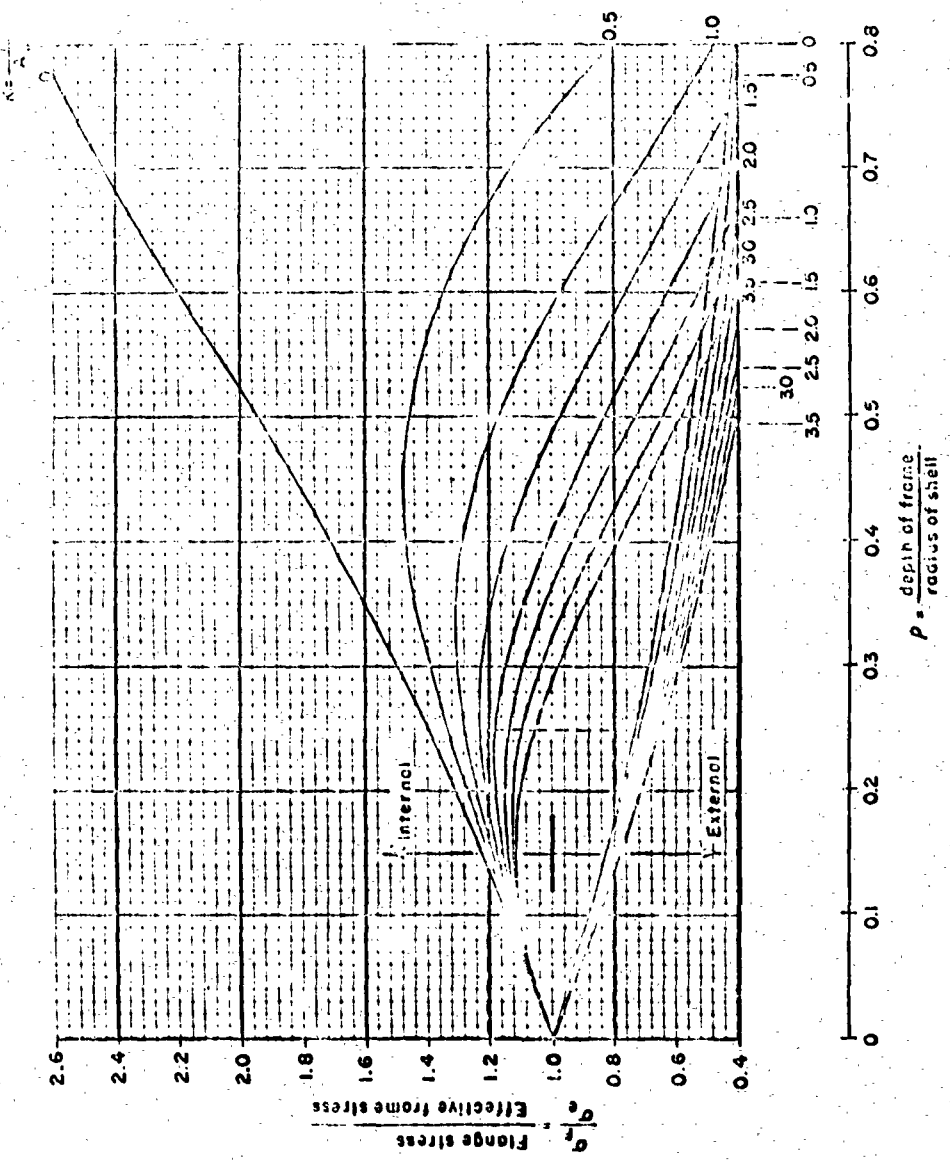


Figure 8 - Plots for Equations (33) and (34), $v = 0.25$



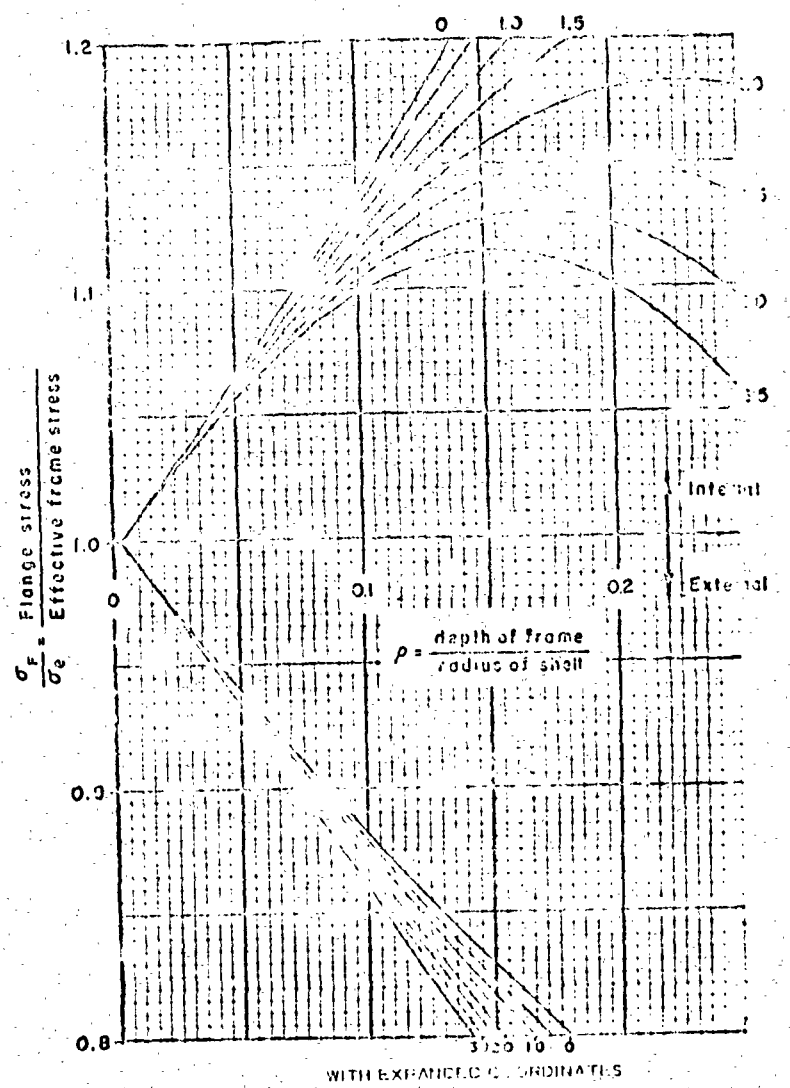
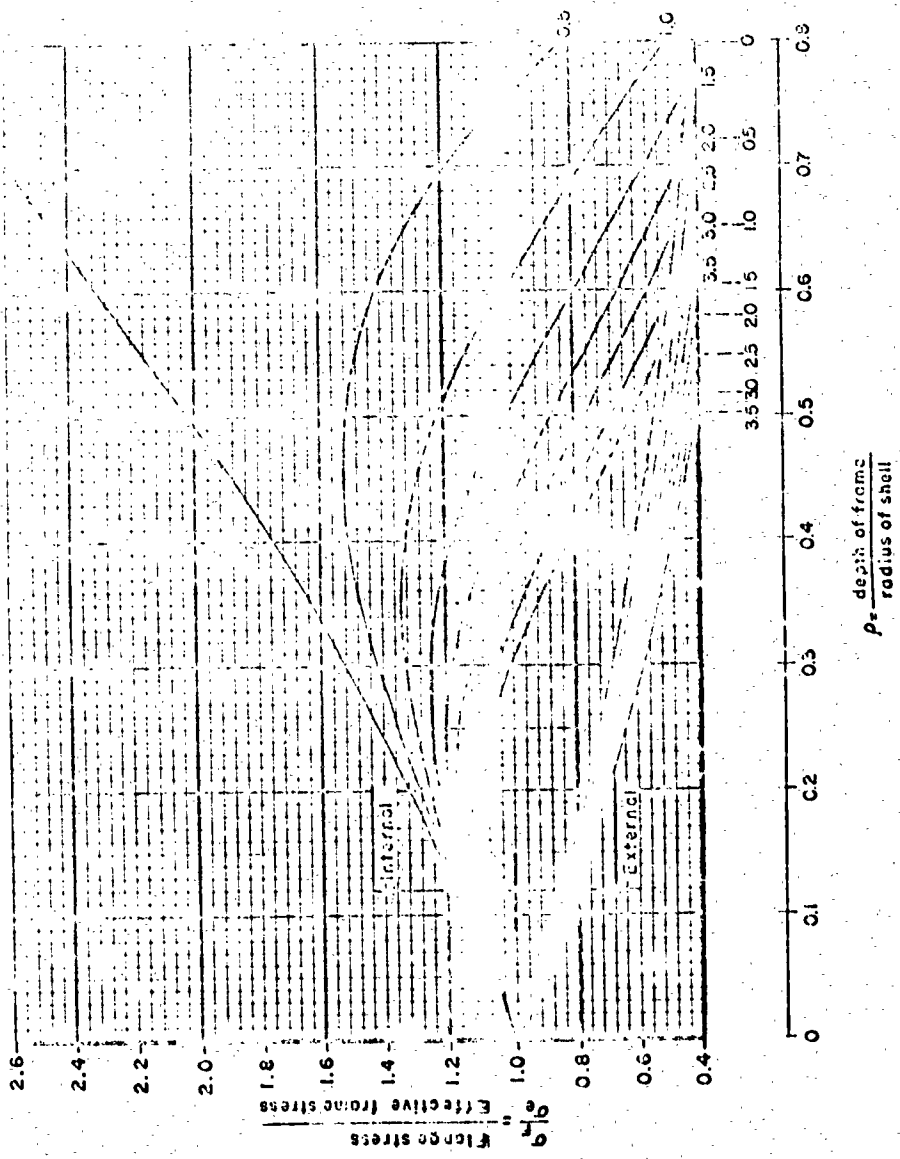


Figure 9 - Plots of Equations (33) and (34), $v = 0.30$



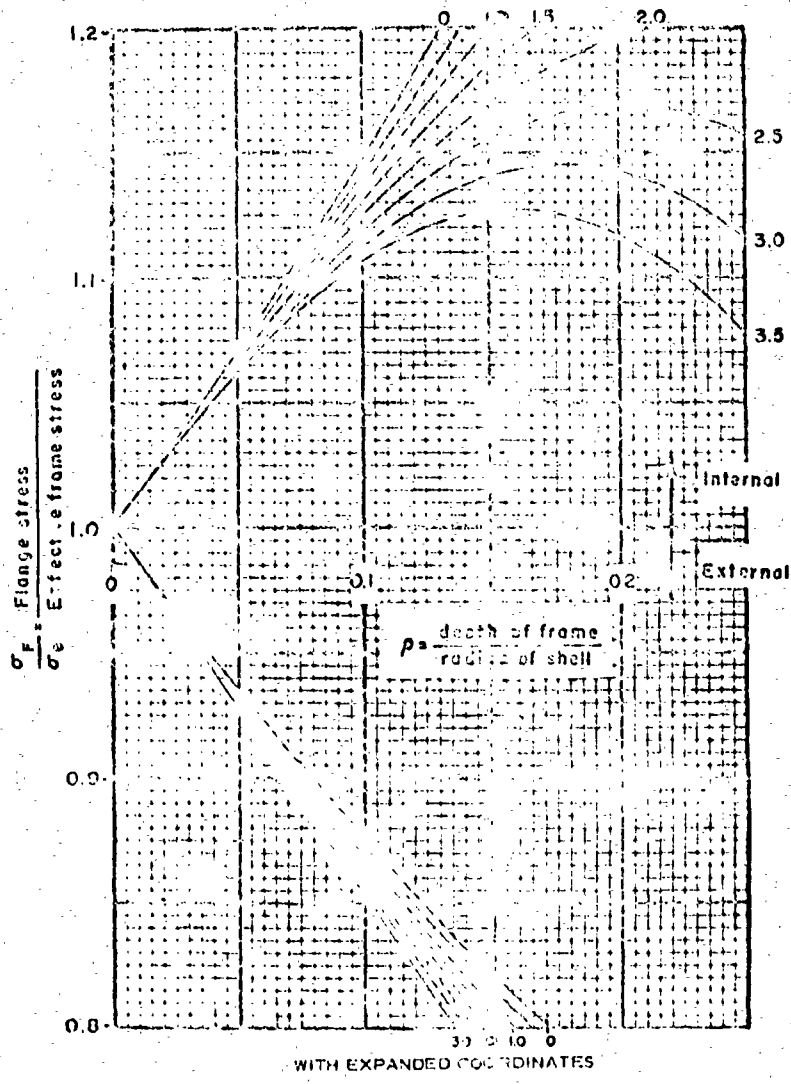


Figure 10 - Plots for Equations (33) and (34), $v = 0.35$